70. D^0-$\overline{D}^0$ Mixing

Revised September 2023 by D.M. Asner (BNL) and A.J. Schwartz (U. of Cincinnati).

The formalism for D^0-$\overline{D}^0$ mixing is closely related to that for CP violation; for further details on the latter, see the note "CP Violation in the Quark Sector" in this *Review*. The time evolution of the D^0–$\overline{D}^0$ system is described by the Schrödinger equation

$$i\frac{\partial}{\partial t}\begin{pmatrix} D^0(t) \\ \overline{D}^0(t) \end{pmatrix} = \left(\mathbf{M} - \frac{i}{2}\mathbf{\Gamma}\right)\begin{pmatrix} D^0(t) \\ \overline{D}^0(t) \end{pmatrix}, \tag{70.1}$$

where the $\mathbf{M}$ and $\mathbf{\Gamma}$ matrices are Hermitian, and CPT invariance requires that $M_{11} = M_{22} \equiv M$ and $\Gamma_{11} = \Gamma_{22} \equiv \Gamma$. The off-diagonal elements of $\mathbf{M}$ and $\mathbf{\Gamma}$ are referred to as the dispersive and absorptive parts, respectively, of the mixing. The mass eigenstates D_1 and D_2 of the Hamiltonian $\mathbf{M}$ - $i\mathbf{\Gamma}/2$ are defined as

$$|D_{1,2}\rangle \;\equiv\; p|D^0\rangle \pm q|\overline{D}^0\rangle\,, \tag{70.2}$$

where normalization imposes $|p|^2 + |q|^2 = 1$. If $p = \pm q$, then the mass eigenstates are CP eigenstates and CP is conserved in mixing. Our phase convention is $CP|D^0\rangle = -|\overline{D}^0\rangle$ and $\mathrm{Arg}(q/p) \in [-\pi/2, \pi/2]$, which imply that, in the absence of CP violation in mixing, D_2 is CP-even and D_1 is CP-odd.

The eigenvalues of $\mathbf{M}$ - $i\mathbf{\Gamma}/2$ are

$$\omega_{1,2} \;=\; \left(M - \frac{i}{2}\Gamma\right) \pm \frac{q}{p}\left(M_{12} - \frac{i}{2}\Gamma_{12}\right) \;\equiv\; m_{1,2} - \frac{i}{2}\Gamma_{1,2}\,, \tag{70.3}$$

where $m_{1,2}$ and $\Gamma_{1,2}$ are real and correspond to the masses and decay widths, respectively, of the $D_{1,2}$ mass eigenstates. As the trace $\Gamma_{11} + \Gamma_{22} = 2\Gamma$ is unchanged by diagonalizing $\mathbf{\Gamma}$, Γ must equal $(\Gamma_1 + \Gamma_2)/2$, the mean decay width. Solving for the eigenstates of the eigenvalues yields

$$\left(\frac{q}{p}\right)^2 = \frac{M_{12}^* - \frac{i}{2}\Gamma_{12}^*}{M_{12} - \frac{i}{2}\Gamma_{12}}\,. \tag{70.4}$$

If CP is conserved in mixing, then $(q/p)^2 = 1$ and M_{12} and Γ_{12} must be real. In this case, the difference in eigenvalues is $\Delta m \equiv m_2 - m_1 = 2M_{12}$ and $\Delta\Gamma \equiv \Gamma_2 - \Gamma_1 = 2\Gamma_{12}$. The signs of Δm and $\Delta\Gamma$ are difficult to predict from theory and thus must be determined experimentally.

We define dimensionless mixing parameters x and y as

$$x \equiv \frac{\Delta m}{\Gamma} \tag{70.5}$$

$$y \equiv \frac{\Delta\Gamma}{2\Gamma}\,. \tag{70.6}$$

These parameters are measured in several ways. The most precise values are obtained by measuring the time dependence of D^0 decays. For all methods, the initial flavor of the D^0 or $\overline{D}^0$ when produced must be determined. The most common method used for this is to reconstruct $D^{*+} \to D^0\pi^+$ or $D^{*-} \to \overline{D}^0\pi^-$ decays; the charge of the accompanying pion (which has low momentum in the lab frame and is often referred to as the "soft" pion) determines the flavor of the neutral D. BABAR and LHCb have also identified the flavor of the neutral D by reconstructing the semileptonic decays $B^+ \to \overline{D}^0\ell^+\nu$, $B^0 \to D^{*-}\ell^+\nu$, $B^- \to D^0\ell^-\nu$, and $\overline{B}^0 \to D^{*+}\ell^-\nu$; in this case the charge of the accompanying lepton determines the D flavor. Both experiments have used both tags together to select "double-tagged" $B \to D^{*\pm}\ell^{\mp}\nu$, $D^{*\pm} \to (D^0, \overline{D}^0)\pi^{\pm}$ decays, which have especially high purity. At e^+e^- collider experiments such as Belle, BABAR, and BESIII, the D flavor can also be determined by fully reconstructing a flavor-specific D decay on the "opposite side" of an event, i.e., recoiling against the signal-side D decay.

At BESIII, where $D\overline{D}$ pairs are produced near their threshold via $e^+e^- \to \psi(3770) \to D^0\overline{D}^0$, there is relatively little background and the purity of opposite-side tagging is equivalent to that achieved using $D^{*\pm}$ decays. However, BESIII operates at a symmetric e^+e^- collider, and the $D\overline{D}$ pairs are produced almost at rest in the lab frame. As a consequence, the D's do not travel any appreciable distance before decaying, and time-dependent analyses are not possible. To overcome this, measurements of mixing at BESIII utilize the quantum coherence of the initial $\psi(3770) \to D^0\overline{D}^0$ state and time-integrated measurements [1–5].

70.1 Time-Dependent Analyses

Our notation is as follows: Cabibbo-favored (CF) decay amplitudes are denoted $\overline{A}_f \equiv \langle f|H|\overline{D}^0\rangle$ and $A_{\overline{f}} \equiv \langle \overline{f}|H|D^0\rangle$; i.e, the final state is $f = K^+\ell^-\nu$, $K^+\pi^-$, $K^+\pi^-\pi^0$, etc. Doubly-Cabibbo-suppressed (DCS) decay amplitudes are denoted $A_f \equiv \langle f|H|D^0\rangle$ and $\overline{A}_{\overline{f}} \equiv \langle \overline{f}|H|\overline{D}^0\rangle$. When discussing decay rates, we neglect constant phase-space factors, which divide out in ratios of rates to common final states.

Starting from a pure $|D^0\rangle$ or $|\overline{D}^0\rangle$ state at $t = 0$, the time-dependent decay rates to "wrong-sign" final states can be written

$$r(t) \equiv \left|\langle f|H|D^0(t)\rangle\right|^2 = \left|\overline{A}_f\right|^2 \left|\frac{q}{p}\right|^2 \left|g_+(t)\,\lambda_f^{-1} + g_-(t)\right|^2 \qquad (70.7)$$

$$\overline{r}(t) \;\equiv\; \left|\langle \overline{f}|H|\overline{D}^0(t)\rangle\right|^2 = \left|A_{\overline{f}}\right|^2 \left|\frac{p}{q}\right|^2 \left|g_+(t)\,\lambda_{\overline{f}} \;+\; g_-(t)\right|^2 , \qquad (70.8)$$

where

$$\lambda_f \;\equiv\; \frac{q}{p}\frac{\overline{A}_f}{A_f}\,, \quad \lambda_{\overline{f}} \;\equiv\; \frac{q}{p}\frac{\overline{A}_{\overline{f}}}{A_{\overline{f}}}\,, \qquad (70.9)$$

and

$$g_\pm(t) \;=\; \frac{1}{2}\left(e^{-i\omega_1 t} \pm e^{-i\omega_2 t}\right) . \qquad (70.10)$$

A change in convention for the relative phase of D^0 and $\overline{D}^0$ would cancel between q/p and $\overline{A}_f/A_f$ or $\overline{A}_{\overline{f}}/A_{\overline{f}}$, leaving λ_f and $\lambda_{\overline{f}}$ unchanged. For multibody final states, these equations apply separately to each point in phase-space. Integrating over regions of phase-space can lead to enhanced sensitivity to CP violation; see the discussion below on multibody decays and the note "Review of Multibody Charm Analyses" in this *Review*. As the mixing parameters x and y are very small, $r(t)$ and $\overline{r}(t)$ are usually expanded to second order in x and y.

70.2 Semileptonic decays

Consider the final state $f = K^+\ell^-\bar{\nu}_\ell$, where $A_f = \overline{A}_{\overline{f}} = 0$ is an excellent approximation in the Standard Model. The final state f is accessible from a D^0 only via mixing,[1] and the decay rate is

$$r(t) = \left|\overline{A}_f\right|^2 \left|\frac{q}{p}\right|^2 |g_-(t)|^2 \;\approx\; \left|\overline{A}_f\right|^2 \left|\frac{q}{p}\right|^2 \left(\frac{x^2+y^2}{4}\right) (\Gamma t)^2\, e^{-\Gamma t} . \qquad (70.11)$$

[1] There exists a doubly Cabibbo-suppressed amplitude in which the c and $\bar{u}$ quarks exchange a W, and then the resulting d quark (from c) decays semileptonically. We neglect this second-order process.

For $\overline{r}(t)$, q/p is replaced by p/q. In the Standard Model, CP violation in charm mixing is small and $|q/p| \approx 1$. In the limit of CP conservation, $r(t) = \overline{r}(t)$, and the time-integrated mixed decay rate relative to the time-integrated unmixed decay rate for semileptonic decays is

$$\frac{\displaystyle\int_0^\infty r(t)\, dt}{\displaystyle\int_0^\infty \left|\overline{A}_f\right|^2 e^{-\Gamma t}\, dt} \;=\; \frac{x^2+y^2}{2} \;\equiv\; R_M\,. \tag{70.12}$$

Table 70.1 summarizes results for R_M from semileptonic decays. The world average from the Heavy Flavor Averaging Group (HFLAV) [6] is $R_M = (1.30 \pm 2.69) \times 10^{-4}$.

Table 70.1: Results for $R_M = (x^2+y^2)/2$ in D^0 semileptonic decays. The HFLAV average assumes statistical and systematic uncertainties are uncorrelated. When a single uncertainty is listed, that corresponds to statistical and systematic uncertainties combined. The measurements with an asterisk (*) have been superseded and thus are not included in the HFLAV average.

Year	Experiment	Final state(s)	R_M ($\times 10^{-3}$)	90% C.L. ($\times 10^{-3}$)
2008	Belle (492 fb^{-1}) [7]	$K^{(*)+}e^-\overline{\nu}_e$	$0.13\pm0.22\pm0.20$	< 0.61
2007	BABAR (344 fb^{-1}) [8]	$K^{(*)+}e^-\overline{\nu}_e$	$0.04\,^{+0.70}_{-0.60}$	$(-1.3, 1.2)$
2005	CLEO (9.0 fb^{-1}) [9]	$K^{(*)+}e^-\overline{\nu}_e$	$1.6\pm2.9\pm2.9$	< 7.8
1996	E791 (2×10^{10} evts) [10]	$K^+\ell^-\overline{\nu}_\ell$	$1.1\,^{+3.0}_{-2.7}\,^{+0.0}_{-0.1}$	< 5.0
	HFLAV Average [6]		$\mathbf{0.130 \pm 0.269}$	
2005*	Belle (253 fb^{-1}) [11]	$K^{(*)+}e^-\overline{\nu}_e$	$0.02\pm0.47\pm0.14$	< 1.0
2004*	BABAR (87 fb^{-1}) [12]	$K^{(*)+}e^-\overline{\nu}_e$	$2.3\pm1.2\pm0.4$	< 4.2

70.3 Wrong-sign decays to hadronic non-CP eigenstates

Consider the final state $f = K^+\pi^-$, i.e., $A_{\overline{f}}$ and $\overline{A}_f$ are CF, A_f and $\overline{A}_{\overline{f}}$ are DCS. Because CF and DCS decays proceed via tree-level amplitudes, and such amplitudes involve only the first two quark generations, direct CP violation is negligible[2]. The ratios of decay amplitudes can be written

$$\frac{A_f}{\overline{A}_f} \;=\; -\sqrt{R_D^+}\,e^{-i\delta_f} \qquad\qquad \frac{\overline{A}_{\overline{f}}}{A_{\overline{f}}} \;=\; -\sqrt{R_D^-}\,e^{-i\delta_f}\,, \tag{70.13}$$

where δ_f is the strong phase difference between the DCS and CF amplitudes. The minus sign originates from the weak phase difference between the amplitudes, specifically, the relative minus sign between V_{us} and V_{cd} (which produces a relative minus sign between $V_{cs}^*V_{ud}$ and $V_{us}^*V_{cd}$). The parameters R_D^+ and R_D^- are the ratios of the DCS decay rate to the CF decay rate. From the relevant CKM matrix elements, one estimates R_D^+, $R_D^- \sim \tan^4\theta_c$, where θ_c is the Cabibbo angle.

With the parameterization of Eq. (70.13), Eq. (70.9) becomes

$$\lambda_f^{-1} \;=\; \frac{p}{q}\frac{A_f}{\overline{A}_f} = -\sqrt{R_D^+}\left|\frac{p}{q}\right| e^{-i(\delta_f+\phi)} \tag{70.14}$$

$$\lambda_{\overline{f}} \;=\; \frac{q}{p}\frac{\overline{A}_{\overline{f}}}{A_{\overline{f}}} = -\sqrt{R_D^-}\left|\frac{q}{p}\right| e^{-i(\delta_f-\phi)}\,, \tag{70.15}$$

where $\phi = \mathrm{Arg}(q/p)$. The weak phase ϕ is independent of the final state f and is often referred to as "universal." For convenience, we define the mean decay rate $R_D \equiv (R_D^+ + R_D^-)/2$, and the decay rate asymmetry $A_D \equiv (R_D^+ - R_D^-)/(R_D^+ + R_D^-)$.

[2] For two quark generations, the weak phases can be defined to eliminate all weak-phase differences.

With these definitions, we expand the decay rates in Eqs. (70.7) and (70.8) to second order in the small mixing parameters x and y to obtain [13, 14]:

$$r(t) = \left|\overline{A}_f\right|^2 e^{-\Gamma t}\left[R_D(1+A_D) \;+\; \sqrt{R_D(1+A_D)}\left|\frac{q}{p}\right| y'_+(\Gamma t) + \;\left|\frac{q}{p}\right|^2 \frac{(x'^2_+ + y'^2_+)}{4}(\Gamma t)^2\right] \quad (70.16)$$

and

$$\overline{r}(t) = \left|A_{\overline{f}}\right|^2 e^{-\Gamma t}\left[R_D(1-A_D) \;+\; \sqrt{R_D(1-A_D)}\left|\frac{p}{q}\right| y'_-(\Gamma t) + \;\left|\frac{p}{q}\right|^2 \frac{(x'^2_- + y'^2_-)}{4}(\Gamma t)^2\right], \quad (70.17)$$

where

$$x'_\pm = x\cos(\delta_f \pm \phi) + y\sin(\delta_f \pm \phi) \quad (70.18)$$

$$y'_\pm = y\cos(\delta_f \pm \phi) - x\sin(\delta_f \pm \phi)\,. \quad (70.19)$$

Defining the "strong-phase-rotated" mixing parameters

$$x' \equiv x\cos\delta_f \;+\; y\sin\delta_f \quad (70.20)$$

$$y' \equiv y\cos\delta_f \;-\; x\sin\delta_f \quad (70.21)$$

gives

$$x'_\pm = x'\cos\phi \;\pm\; y'\sin\phi \quad (70.22)$$

$$y'_\pm = y'\cos\phi \;\mp\; x'\sin\phi\,, \quad (70.23)$$

i.e., $x'_\pm$ and $y'_\pm$ are obtained from x', y' via an additional "weak-phase rotation." To summarize, parameters (x', y') are the mixing parameters (x, y) rotated by the strong phase δ_f, and parameters $(x'_\pm, y'_\pm)$ are the parameters (x', y') rotated by the weak phase $+\phi$ for D^0 decays and $-\phi$ for $\overline{D}^0$ decays. Note that $x'^2_+ + y'^2_+ \;=\; x'^2_- + y'^2_- \;=\; x'^2 + y'^2 \;=\; x^2 + y^2$. In Eqs. (70.16) and (70.17), a fourth term $R_D(1 \pm A_D)(x^2_\pm - y^2_\pm)(\Gamma t)^2/4$ has been dropped, as it is negligible relative to the other terms for the range of decay times measured by experiments.

Comparing Eqs. (70.16) and (70.17), one sees that $r(t) \neq \overline{r}(t)$ and CP is violated if either $A_D \neq 0$, $|q/p| \neq 1$, or $\phi \neq 0$. These three inequalities correspond, respectively, to the three types of CP violation: in the decay amplitudes ($R^+_D \neq R^-_D$); in the mixing; and due to interference between a mixed decay amplitude (i.e., mixing is followed by decay) and an unmixed decay amplitude. Whereas CP violation in the decay amplitudes is parameterized by A_D, CP violation in mixing is parameterized by $A_M \equiv (|q/p| - |p/q|)/(|q/p| + |p/q|)$.

In the limit of CP conservation, $A_D = 0$, $|q/p| = 1$, and $\phi = 0$. In this case

$$r(t) = \;\overline{r}(t) = \;\left|A_{\overline{f}}\right|^2 e^{-\Gamma t}\left[R_D + \sqrt{R_D}\,y'(\Gamma t) + \frac{x'^2 + y'^2}{4}(\Gamma t)^2\right], \quad (70.24)$$

and the total number of $D^0 \to f$ decays divided by the total number of $D^0 \to \bar{f}$ decays is

$$R \;=\; \frac{\int_0^\infty r(t)\,dt}{\int_0^\infty \left|A_{\overline{f}}\right|^2 e^{-\Gamma t}\,dt} \;=\; R_D + \sqrt{R_D}\,y' + \frac{x'^2 + y'^2}{2}\,. \quad (70.25)$$

The ratio R is more straightforward to measure than $r(t)$ or $\bar{r}(t)$, as there is no decay-time dependence. In Table 70.2 we report measurements of R, R_D, and A_D in $D^0 \to K^+\pi^-$ decays normalized to $D^0 \to K^-\pi^+$ decays, and results from HFLAV [15] obtained from a global fit to all relevant data that allows for both mixing and CP violation (see Section 70.7). The experiments typically perform a single fit for parameters R_D, x'^2, and y'; results for x'^2 and y' are listed in Table 70.3. Allowing for CP violation, the experiments measure parameters (R_D^+, x'^2_+, y'_+) and (R_D^-, x'^2_-, y'_-) [or equivalently (R_D, A_D) instead of (R_D^+, R_D^-)] by separately fitting the $D^0 \to K^+\pi^-$ and $\overline{D}^0 \to K^-\pi^+$ event samples.

Table 70.2: Results for R, R_D, and A_D as measured using $D^0 \to K^\pm\pi^\mp$ decays. When a single uncertainty is listed, that corresponds to statistical and systematic uncertainties combined. The measurements with an asterisk (*) have been superseded and thus are not included in the HFLAV global fit (Section 70.7). The measurements with a dagger (†) are not included in the HFLAV global fit due to much poorer precision.

Year	Experiment	$R\,(\times 10^{-3})$	$R_D\,(\times 10^{-3})$	$A_D\,(\%)$
2018	LHCb (5.0 fb^{-1} D^* tag) [16]	—	3.454 ± 0.031	-0.01 ± 0.91
2017	LHCb (3.0 fb^{-1} $B+D^*$ double tag) [17]	—	3.48 ± 0.10	-3.15 ± 3.31
2014	Belle (976 fb^{-1}) [18]	3.86 ± 0.06	3.53 ± 0.13	—
2013	CDF (9.6 fb^{-1}) [19]	4.30 ± 0.05	3.51 ± 0.35	—
2007	BABAR (384 fb^{-1}) [20]	$3.53\pm0.08\pm0.04$	$3.03\pm0.16\pm0.10$	$-2.1\pm5.2\pm1.5$
	HFLAV Fit Result [15]		$\mathbf{3.434 \pm 0.019}$	$\mathbf{-0.70 \pm 0.36}$
2013b*	LHCb (3.0 fb^{-1} D^* tag) [21]	—	3.568 ± 0.066	-0.7 ± 1.9
2013a*	LHCb (1.0 fb^{-1}) [22]	4.25 ± 0.04	3.52 ± 0.15	—
2008*	CDF (1.5 fb^{-1}) [23]	4.15 ± 0.10	3.04 ± 0.55	—
2006*	Belle (400 fb^{-1}) [24]	$3.77\pm0.08\pm0.05$	3.64 ± 0.18	2.3 ± 4.7
2005†	FOCUS (234 evts) [25]	$4.29\,^{+0.63}_{-0.61}\pm0.27$	$5.17\,^{+1.47}_{-1.58}\pm0.76$	$13\,^{+33}_{-25}\pm10$
2000†	CLEO (9.0 fb^{-1}) [26]	$3.32\,^{+0.63}_{-0.65}\pm0.40$	$4.8\pm1.2\pm0.4$	$-1\,^{+16}_{-17}\pm1$
1998†	E791 (5643 evts) [27]	$6.8\,^{+3.4}_{-3.3}\pm0.7$	—	—

Extraction of the mixing parameters x and y from measurements of x' and y' requires knowledge of the strong phase difference $\delta_{K\pi}$. This can be determined from the decay rates of $D_\pm \to K^+\pi^-$, where D_+ (D_-) denotes the CP-even (CP-odd) eigenstate. Since $|D_\pm\rangle = (|D^0\rangle \mp |\overline{D}^0\rangle)/\sqrt{2}$,

$$\sqrt{2}\,A(D_\pm \to K^+\pi^-) \;=\; A(D^0 \to K^+\pi^-) \mp A(\overline{D}^0 \to K^+\pi^-)\,. \tag{70.26}$$

Squaring this amplitude and using Eq. (70.13) yields the relation

$$\cos\delta_{K\pi} \;=\; \frac{|A(D_+ \to K^+\pi^-)|^2 - |A(D_- \to K^+\pi^-)|^2}{2\,|A(D^0 \to K^+\pi^-)|\,|A(\overline{D}^0 \to K^+\pi^-)|}\,. \tag{70.27}$$

Measuring the right-hand side is possible if one can identify pure D_+, D_-, D^0, and $\overline{D}^0$ initial states. This is accomplished at CLEOc and BESIII utilizing the processes $e^+e^- \to \psi(3770) \to \overline{D}^0 D^0 \to (f_{CP})(K^+\pi^-)$, or $\psi(3770) \to \overline{D}^0 D^0 \to (f_{\overline{D}^0})(K^+\pi^-)$, where f_{CP} denotes a CP-specific final state, and $f_{\overline{D}^0}$ denotes a $\overline{D}^0$-flavor-specific final state. In the first case, quantum coherence and CP symmetry ensures that the $K^+\pi^-$ state originates from a neutral D with CP opposite that of f_{CP}. In the second case, at the time when the $\overline{D}^0$ decays, the opposite side is D^0. However, it can potentially mix to $\overline{D}^0$ before decaying to $K^+\pi^-$, and this introduces some dependence on the mixing parameters x and y. This dependence is seen explicitly in the observable

$$A^{CP}_{K\pi} \;\equiv\; \frac{|A(D_- \to K^-\pi^+)|^2 - |A(D_+ \to K^-\pi^+)|^2}{|A(D_- \to K^-\pi^+)|^2 + |A(D_+ \to K^-\pi^+)|^2}\,. \tag{70.28}$$

Table 70.3: Results for x'^2 and y', as measured using $D^0 \to K^\pm\pi^\mp$ decays. When a single uncertainty is listed, that corresponds to statistical and systematic uncertainties combined. The measurements with an asterisk (*) have been superseded and thus are not included in the HFLAV global fit. The measurements with a dagger (†) are not included in the HFLAV global fit due to much poorer precision. All confidence limits and intervals correspond to 95% C.L. The Belle 2006 results restrict x'^2 to the physical region. The BABAR confidence intervals are obtained from the fit, whereas Belle uses a Feldman-Cousins method, and CDF uses a Bayesian method.

Year	Experiment	No CP violation		Allowing for CP violation	
		x'^2 ($\times 10^{-3}$)	y' (%)	x'^2 ($\times 10^{-3}$)	y' (%)
2018	LHCb (5.0 fb^{-1} D^* tag) [16]	0.039 ± 0.027	0.528 ± 0.052	D^0: 0.061 ± 0.037 $\overline{D}^0$: 0.016 ± 0.039	0.501 ± 0.074 0.554 ± 0.074
2017	LHCb (3.0 fb^{-1} $B+D^*$ double tag) [17]	0.028 ± 0.310	0.46 ± 0.37	D^0: -0.019 ± 0.447 $\overline{D}^0$: 0.079 ± 0.433	0.581 ± 0.526 0.332 ± 0.523
2014	Belle (976 fb^{-1}) [18]	0.09 ± 0.22	0.46 ± 0.34	—	—
2013	CDF (9.6 fb^{-1}) [19]	0.08 ± 0.18	0.43 ± 0.43	—	—
2007	BABAR (384 fb^{-1}) [20]	-0.22 ± 0.37	0.97 ± 0.54	D^0: -0.24 ± 0.52 $\overline{D}^0$: -0.20 ± 0.50	0.98 ± 0.78 0.96 ± 0.75
2006	Belle (400 fb^{-1}) [24]	$\left(0.18\,^{+0.21}_{-0.23}\right)^*$	$\left(0.06\,^{+0.40}_{-0.39}\right)^*$	< 0.72	$-2.8 < y' < 2.1$
2013b*	LHCb (3.0 fb^{-1} D^* tag) [21]	0.055 ± 0.049	0.48 ± 0.10	D^0: 0.049 ± 0.070 $\overline{D}^0$: 0.060 ± 0.068	0.51 ± 0.14 0.45 ± 0.14
2013a*	LHCb (1.0 fb^{-1}) [22]	-0.09 ± 0.13	0.72 ± 0.24	—	—
2008*	CDF (1.5 fb^{-1}) [23]	-0.12 ± 0.35	0.85 ± 0.76	—	—
2005†	FOCUS (234 evts) [25]	< 8.3	$-7.2 < y' < 4.1$	< 8.0	$-11.2 < y' < 6.7$
2000†	CLEO (9.0 fb^{-1}) [26]	0.00 ± 0.23	$-2.3\,^{+1.3}_{-1.4}$	0.00 ± 0.23	$-2.5\,^{+1.4}_{-1.6}$
1998†	E791 (5643 evts) [27]	< 17	< 13	—	—

To lowest order in the mixing parameters [28],

$$A^{CP}_{K\pi} = \frac{2\sqrt{R_D}\cos\delta_{K\pi} + y}{1+R}, \tag{70.29}$$

where R is defined in Eq. (70.25). Such measurements are discussed in Section 70.5.

70.3.1 *Wrong-sign decays to multibody final states*

For multibody final states, Eqs. (70.13)-(70.25) apply to each point in phase-space.[3] Although x and y do not vary across phase-space, knowledge of the resonant substructure is needed to determine the strong phase difference δ from point to point to extract x and y. Alternatively, experimental knowledge of the strong phase difference between D^0 and $\overline{D}^0$ decay amplitudes across phase space [29] allow one to determine x and y independent of a decay model of resonant substructure. This phase information can be measured at the charm threshold, where CLEO-c and BESIII took data.

A time-dependent analysis at BABAR [30,31] of $D^0 \to K^+\pi^-\pi^0$ decays, relative to CF $\overline{D}^0 \to K^+\pi^-\pi^0$ decays, determined the strong phase variation across the Dalitz plot and reported $x'' =$

[3]However, if the decay amplitudes involve the third generation, then $A_f/\overline{A}_f$ and $\overline{A}_{\overline{f}}/A_{\overline{f}}$ in Eq. (70.13) also have weak phase differences. However, this phase difference is estimated to be negligible for the sensitivity of current and foreseeable future experimental measurements.

$(2.61\,^{+0.57}_{-0.68} \pm 0.39)\%$ and $y'' = (-0.06\,^{+0.55}_{-0.64} \pm 0.34)\%$. These mixing parameters are defined as

$$x'' = x\cos\delta_{K\pi\pi^0} + y\sin\delta_{K\pi\pi^0} \tag{70.30}$$

$$y'' = y\cos\delta_{K\pi\pi^0} - x\sin\delta_{K\pi\pi^0}\,, \tag{70.31}$$

in analogy with x', y', and $\delta_{K\pi}$ of Eqs. (70.20) and (70.21). Here, $\delta_{K\pi\pi^0}$ is the strong phase difference between the amplitudes $A(D^0 \to K^+\rho^-)$ and $A(\overline{D}^0 \to K^+\rho^-)$. The phase difference $\delta_{K\pi\pi^0}$ can be determined in a manner similar to that for $\delta_{K\pi}$: by using Eq. (70.27) and quantum-correlated measurements of the branching fractions $B(D_+ \to K^+\rho^-)$, $B(D_- \to K^+\rho^-)$, $B(D^0 \to K^+\rho^-)$, and

Table 70.4: Results from time-dependent multibody analyses. The errors are statistical, systematic, and, when a third error is listed, due to the decay-model, respectively. The measurement with an asterisk (*) has been superseded and thus is not included in the HFLAV global fit. The measurement with a dagger (†) is not included in the HFLAV global fit due to poorer precision. The 2019 LHCb result utilizes strong-phase measurements from CLEO-c [32] and thus is decay-model independent. The 2019–2023 LHCb fits determine *CP*-violating parameters Δx and Δy; the translation of these parameters to $|q/p|$ and ϕ is given in Ref. [33].

No *CP* Violation

Year	Experiment	Final state(s)	x ($\times 10^{-3}$)	y ($\times 10^{-3}$)
2023	LHCb (5.4 fb^{-1} B tag) [34]	$K^0_S\pi^+\pi^-$	$4.29 \pm 1.48 \pm 0.26$	$12.61 \pm 3.12 \pm 0.83$
2021	LHCb (5.4 fb^{-1} D^* tag) [35]	$K^0_S\pi^+\pi^-$	$3.97 \pm 0.46 \pm 0.29$	$4.59 \pm 1.20 \pm 0.85$
2019	LHCb (3.0 fb^{-1} B, D^* tags) [36]	$K^0_S\pi^+\pi^-$	$2.7 \pm 1.6 \pm 0.4$	$7.4 \pm 3.6 \pm 1.1$
2016	LHCb (1.0 fb^{-1} D^* tag) [37]	$K^0_S\pi^+\pi^-$	$-8.6 \pm 5.3 \pm 1.7$	$0.3 \pm 4.6 \pm 1.3$
2016	BABAR (468 fb^{-1}) [38]	$\pi^+\pi^-\pi^0$	$15 \pm 12 \pm 6$	$2 \pm 9 \pm 5$
2014	Belle (921 fb^{-1}) [39]	$K^0_S\pi^+\pi^-$	$5.6 \pm 1.9\,^{+0.3}_{-0.9}\,^{+0.6}_{-0.9}$	$3.0 \pm 1.5\,^{+0.4}_{-0.5}\,^{+0.3}_{-0.6}$
2010	BABAR (469 fb^{-1}) [40]	$K^0_S\pi^+\pi^-$ $K^0_S K^+K^-$	$1.6 \pm 2.3 \pm 1.2 \pm 0.8$	$5.7 \pm 2.0 \pm 1.3 \pm 0.7$
2007*	Belle (540 fb^{-1}) [41]	$K^0_S\pi^+\pi^-$	$8.0 \pm 2.9\,^{+0.9}_{-0.7}\,^{+1.0}_{-1.4}$	$3.3 \pm 2.4\,^{+0.8}_{-1.2}\,^{+0.6}_{-0.8}$
2005†	CLEO (9.0 fb^{-1}) [42]	$K^0_S\pi^+\pi^-$	$19\,^{+32}_{-33} \pm 4 \pm 4$	$-14 \pm 24 \pm 8 \pm 4$

With *CP* Violation

Year	Experiment	Final state(s)	$\lvert q/p\rvert$	ϕ
2023	LHCb (5.4 fb^{-1}) [34]	$K^0_S\pi^+\pi^-$	$\Delta x \times 10^3 =$ $-0.77 \pm 0.93 \pm 0.28$	$\Delta y \times 10^3 =$ $3.01 \pm 1.92 \pm 0.26$
2021	LHCb (5.4 fb^{-1}) [35]	$K^0_S\pi^+\pi^-$	0.996 ± 0.052 $\Delta x \times 10^3 =$ $-0.27 \pm 0.18 \pm 0.01$	$(3.2\,^{+2.7}_{-2.9})^\circ$ $\Delta y \times 10^3 =$ $0.20 \pm 0.36 \pm 0.13$
2019	LHCb (3.0 fb^{-1}) [36]	$K^0_S\pi^+\pi^-$	$1.05\,^{+0.22}_{-0.17}$ $\Delta x \times 10^3 =$ $-0.53 \pm 0.70 \pm 0.22$	$(-5.2\,^{+6.3}_{-9.2})^\circ$ $\Delta y \times 10^3 =$ $0.6 \pm 1.6 \pm 0.3$
2014	Belle (921 fb^{-1}) [39]	$K^0_S\pi^+\pi^-$	$0.90\,^{+0.16}_{-0.15}\,^{+0.05}_{-0.04}\,^{+0.06}_{-0.05}$	$(-6 \pm 11 \pm 3\,^{+3}_{-4})^\circ$
2007*‡	Belle (540 fb^{-1}) [41]	$K^0_S\pi^+\pi^-$	$0.86\,^{+0.30}_{-0.29}\,^{+0.06}_{-0.03} \pm 0.08$	$(-14\,^{+16}_{-18}\,^{+5}_{-3}\,^{+2}_{-4})^\circ$

‡This result allows for all types of *CP* violation and is superseded by Ref. [39], which assumes no direct *CP* violation in CF or DCS decays.

$B(\overline{D}^0 \to K^+\rho^-)$ in $e^+e^- \to \psi(3770)$ events.

For the decay modes D^0 and $\overline{D}^0 \to K^+\pi^-\pi^+\pi^-$, Belle measured $R = (0.324 \pm 0.008 \pm 0.007)\%$ [43]. Subsequently, a phase-space-integrated analysis from LHCb [44] measured the product of a "coherence factor" $R_D^{K3\pi}$ and the strong-phase-rotated mixing parameter $y''_{K3\pi}$. This measurement resulted in an observation of charm mixing with 8.2σ significance.

Both the sign and magnitude of x and y without strong phases entering or sign ambiguity can be determined by measuring the time-dependent resonant substructure of multibody D^0 decays to self-conjugate final states [41, 42]. For such decays, e.g., $D^0 \to K_S^0\pi^+\pi^-$, the DCS and CF decay amplitudes populate the same Dalitz plot, which allows for direct measurement of the strong phase difference. Belle [39, 41], BABAR [40], and CLEO [45] have measured the overall phase difference between $D^0 \to K^*(892)^-\pi^+$ and $D^0 \to K^*(892)^+\pi^-$ to be $[173.9 \pm 0.7$ (stat. only)$]^\circ$, $[177.6 \pm 1.1$ (stat. only)$]^\circ$, and $[189 \pm 10 \pm 3\,^{+15}_{-5}]^\circ$, respectively. These results are close to the 180° expected from Cabibbo factors, i.e., the relative minus sign between $V_{cs}^*V_{ud}$ and $V_{us}^*V_{cd}$; thus they indicate a small strong phase. Four LHCb measurements [34–37] of x, y using $D^0 \to K_S^0\pi^+\pi^-$ decays are decay-model independent, as the model of resonances in the intermediate state is replaced by strong-phase measurements from CLEO-c [32] and BESIII [46]. Table 70.4 summarizes results from time-dependent analyses of self-conjugate multibody final states. World average values for the measurements listed are given later, as a result of the HFLAV global fit.

With regard to resonant substructure in $D^0 \to K_S^0\pi^+\pi^-$ decays, Belle [39, 41] measured the relative strong phase (statistical errors only) and the ratio R (central values only) of the DCS fit fraction relative to the CF fit fraction for five excited K states: $K^*(892)^+\pi^-$, $K_0^*(1430)^+\pi^-$, $K_2^*(1430)^+\pi^-$, $K^*(1410)^+\pi^-$, and $K^*(1680)^+\pi^-$. Similarly, BABAR [40, 47, 48] reported central values of R for $K^*(892)^+\pi^-$, $K_0^*(1430)^+\pi^-$, and $K_2^*(1430)^+\pi^-$. The systematic uncertainties on R are not evaluated. Large differences in R are observed among these final states, which indicates significant hadronic effects.

70.4 Decays to *CP* Eigenstates

When the final state f is a CP eigenstate, there is no distinction between f and $\overline{f}$. Thus $A_f = A_{\overline{f}}$ and $\overline{A}_{\overline{f}} = \overline{A}_f$. We denote final states with CP eigenvalues ±1 by $f_\pm$. Decays to CP eigenstates proceed mainly via singly Cabibbo-suppressed amplitudes. Such amplitudes can contain internal loops and thus involve the third quark generation; in this manner a weak phase would appear in the decay amplitude, leading to direct CP violation. However, such internal loop amplitudes are suppressed, and the presence of a weak phase is often neglected.

The mixing parameter y may be measured by comparing the rate for D^0 decays to CP eigenstates such as K^+K^- with the rate to flavor eigenstates such as $K^-\pi^+$ [14]. If decays to K^+K^- have a shorter effective lifetime than those to $K^-\pi^+$, then $\Gamma_+ > \Gamma_-$, or, since CP violation is very small, $\Gamma_2 > \Gamma_1$ and y is positive. For small mixing ($x, y \ll 1$), the decay rates for $D^0 \to f_\pm$ and $\overline{D}^0 \to f_\pm$ have an approximately exponential time dependence:

$$r_\pm(t) \propto \exp(-\Gamma_\pm t) \qquad (70.32)$$

$$\overline{r}_\pm(t) \propto \exp(-\overline{\Gamma}_\pm t)\,, \qquad (70.33)$$

where the effective decay widths are given by

$$\Gamma_\pm = \Gamma\left(1 \pm \left|\frac{q}{p}\right|(y\cos\phi - x\sin\phi)\right) \qquad (70.34)$$

$$\overline{\Gamma}_\pm = \Gamma\left(1 \pm \left|\frac{p}{q}\right|(y\cos\phi + x\sin\phi)\right)\,. \qquad (70.35)$$

Table 70.5: Results for y_{CP} and A_Γ from D^0 decays to CP eigenstates. When a single uncertainty is listed, that corresponds to statistical and systematic uncertainties combined. The measurements with an asterisk (*) have been superseded.

Year	Experiment	Final state(s)	y_{CP} (%)	A_Γ ($\times 10^{-3}$)
2022‡	LHCb (6 fb^{-1} D^* tag) [49]	$K^+K^- + \pi^+\pi^-$	$0.696 \pm 0.026 \pm 0.013$	—
2021	LHCb (8.4 fb^{-1} B, D^* tags) [50]	$K^+K^- + \pi^+\pi^-$	—	$0.10 \pm 0.11 \pm 0.03$
2021	LHCb (6 fb^{-1} D^* tag) [50]	$K^+K^- + \pi^+\pi^-$	—	$0.27 \pm 0.13 \pm 0.03$
2021	LHCb (6 fb^{-1} D^* tag) [50]	K^+K^-	—	$0.23 \pm 0.15 \pm 0.03$
2021	LHCb (6 fb^{-1} D^* tag) [50]	$\pi^+\pi^-$	—	$0.40 \pm 0.28 \pm 0.04$
2020	Belle (976 fb^{-1}) [51]	$K^0_S\,\omega$	$0.96 \pm 0.91^{+0.64}_{-0.62}$	—
2019	LHCb (3 fb^{-1} B tag) [52]	$K^+K^- + \pi^+\pi^-$	$0.57 \pm 0.13 \pm 0.09$	—
2017	LHCb (3 fb^{-1} D^* tag) [53]	$K^+K^- + \pi^+\pi^-$	—	$-0.13 \pm 0.28 \pm 0.10$
2017	LHCb (3 fb^{-1} D^* tag) [53]	K^+K^-	—	$-0.30 \pm 0.32 \pm 0.10$
2017	LHCb (3 fb^{-1} D^* tag) [53]	$\pi^+\pi^-$	—	$0.46 \pm 0.58 \pm 0.12$
2016	Belle (976 fb^{-1}) [54]	$K^+K^- + \pi^+\pi^-$	$1.11 \pm 0.22 \pm 0.09$	$-0.3 \pm 2.0 \pm 0.7$
2015	LHCb (3 fb^{-1} B tag) [55]	$K^+K^- + \pi^+\pi^-$	—	-1.25 ± 0.73
2015	LHCb (3 fb^{-1} B tag) [55]	K^+K^-	—	$-1.34 \pm 0.77^{+0.26}_{-0.34}$
2015	LHCb (3 fb^{-1} B tag) [55]	$\pi^+\pi^-$	—	$-0.92 \pm 1.45^{+0.25}_{-0.33}$
2015	BES III (2.9 fb^{-1}) [56]	$\begin{cases} K^+K^-,\ \pi^+\pi^- \\ K^0_S\,\pi^0,\ K^0_S\,\pi^0\pi^0 \\ K^0_S\,\eta,\ K^0_S\,\omega \end{cases}$	$-2.0 \pm 1.3 \pm 0.7$	—
2014	CDF (9.7 fb^{-1}) [57]	$K^+K^- + \pi^+\pi^-$	—	-1.2 ± 1.2
2014	CDF (9.7 fb^{-1}) [57]	K^+K^-	—	$-1.9 \pm 1.5 \pm 0.4$
2014	CDF (9.7 fb^{-1}) [57]	$\pi^+\pi^-$	—	$-0.1 \pm 1.8 \pm 0.3$
2012	BABAR (468 fb^{-1}) [58]	$K^+K^- + \pi^+\pi^-$	$0.72 \pm 0.18 \pm 0.12$	$0.9 \pm 2.6 \pm 0.6$
2009	Belle (673 fb^{-1}) [59]	$K^0_S\,K^+K^-$	$0.11 \pm 0.61 \pm 0.52$	—
2002	CLEO (9.0 fb^{-1}) [60]	$K^+K^- + \pi^+\pi^-$	$-1.2 \pm 2.5 \pm 1.4$	—
2000	FOCUS (1×10^6 evts) [61]	K^+K^-	$3.42 \pm 1.39 \pm 0.74$	—
1999	E791 (2×10^{10} evts) [62]	K^+K^-	$0.73 \pm 2.89 \pm 1.03$	—
	HFLAV Average [63]		$\mathbf{0.719 \pm 0.113}$	$\mathbf{0.089 \pm 0.113}$
2020*	LHCb (5.4 fb^{-1} B tag) [64]	K^+K^-	—	$-0.43 \pm 0.36 \pm 0.05$
2020*	LHCb (5.4 fb^{-1} B tag) [64]	$\pi^+\pi^-$	—	$0.22 \pm 0.70 \pm 0.08$
2013*	LHCb (1.0 fb^{-1} D^* tag) [65]	K^+K^-	—	$-0.35 \pm 0.62 \pm 0.12$
2013*	LHCb (1.0 fb^{-1} D^* tag) [65]	$\pi^+\pi^-$	—	$0.33 \pm 1.06 \pm 0.14$
2011*§	LHCb (29 pb^{-1} D^* tag) [66]	K^+K^-	$0.55 \pm 0.63 \pm 0.41$	$-5.9 \pm 5.9 \pm 2.1$
2009*	BABAR (384 fb^{-1}) [67]	K^+K^-	$1.16 \pm 0.22 \pm 0.18$	—
2008*	BABAR (384 fb^{-1}) [68]	$K^+K^- + \pi^+\pi^-$	$1.03 \pm 0.33 \pm 0.19$	$2.6 \pm 3.6 \pm 0.8$
2007*	Belle (540 fb^{-1}) [69]	$K^+K^- + \pi^+\pi^-$	$1.31 \pm 0.32 \pm 0.25$	$0.1 \pm 3.0 \pm 1.5$
2003*	BABAR (91 fb^{-1}) [70]	$K^+K^- + \pi^+\pi^-$	$0.8 \pm 0.4^{+0.5}_{-0.4}$	—
2001*	Belle (23.4 fb^{-1}) [71]	K^+K^-	$-0.5 \pm 1.0^{+0.7}_{-0.8}$	—

‡This measurement has sufficient precision that y_{CP} for the normalization channel $D^0 \to K^-\pi^+$ must be accounted for. Thus, the measurement is $y_{CP}(h^+h^-) - y_{CP}(K^-\pi^+)$. HFLAV accounts for this small correction in their global fit.

§This result for y_{CP} is not superseded, but it is not included in the HFLAV average due to having some correlations with the result of Ref. [52] but much worse precision.

Thus, the effective decay rate to a CP eigenstate combining equal numbers of D^0 and $\overline{D}^0$ decays (e.g., an untagged sample with no production asymmetry) is

$$r_\pm(t) \; + \; \overline{r}_\pm(t) \; \propto \; e^{-(1\pm y_{CP})\Gamma t}\,, \tag{70.36}$$

where

$$y_{CP} = \frac{1}{2}\left(\left|\frac{q}{p}\right| + \left|\frac{p}{q}\right|\right) y\cos\phi - \frac{1}{2}\left(\left|\frac{q}{p}\right| - \left|\frac{p}{q}\right|\right) x\sin\phi \tag{70.37}$$

$$\approx y\cos\phi - A_M\, x\sin\phi\,. \tag{70.38}$$

If CP is conserved, $y_{CP} = y$. Most measurements of y_{CP} have used $D^0 \to K^+K^-$ and $D^0 \to \pi^+\pi^-$ decays, which are CP-even, measured relative to $D^0 \to K^-\pi^+$. Belle measured y_{CP} also using $D^0 \to K^0_S\,\omega$ decays [51], which are CP-odd, and $D^0 \to K^0_S\, K^+K^-$ decays [59], which are dominated by the CP-odd final state $K^0_S\,\phi$. Table 70.5 summarizes the current status of measurements.

In addition to y_{CP}, Belle [54], BABAR [58], CDF [57], and LHCb [50, 66] have reported measurements of the decay-rate asymmetry for CP-even final states:

$$A_\Gamma \equiv \frac{\Gamma_+ - \overline{\Gamma}_+}{\Gamma_+ + \overline{\Gamma}_+} \;=\; \frac{(1/\tau_+) - (1/\overline{\tau}_+)}{(1/\tau_+) + (1/\overline{\tau}_+)} \;=\; \frac{\overline{\tau}_+ - \tau_+}{\overline{\tau}_+ + \tau_+} \tag{70.39}$$

$$\approx \frac{1}{2}\left(\left|\frac{q}{p}\right| - \left|\frac{p}{q}\right|\right) y\cos\phi - \frac{1}{2}\left(\left|\frac{q}{p}\right| + \left|\frac{p}{q}\right|\right) x\sin\phi \tag{70.40}$$

$$\approx A_M\, y\cos\phi - x\sin\phi\,. \tag{70.41}$$

If CP is conserved, $A_\Gamma = 0$.

There is a contribution to Eq. (70.41) from direct CP violation, i.e., $|\overline{A}_f/A_f| \neq 1$ [72, 73]. For $f = K^+K^-$ and $\pi^+\pi^-$, this contribution can be estimated from measurements of $A_{CP}(K^+K^-)$ and $A_{CP}(\pi^+\pi^-)$ (see below) and is much smaller than the current uncertainty on A_M; thus we neglect it here. We note that, when averaging A_Γ measurements over K^+K^- and $\pi^+\pi^-$ final states, the contribution from direct CP violation cancels, as it has the same magnitude but opposite signs for K^+K^- and $\pi^+\pi^-$ due to U-spin symmetry [73].

The asymmetry A_Γ is an asymmetry in the full decay widths. An asymmetry in partial widths is referred to as A_{CP} and is final-state dependent:

$$A_{CP} \;\equiv\; \frac{\Gamma(D^0 \to f) - \Gamma(\overline{D}^0 \to \overline{f})}{\Gamma(D^0 \to f) + \Gamma(\overline{D}^0 \to \overline{f})}\,. \tag{70.42}$$

Unlike A_Γ, which is measured by fitting decay time distributions, A_{CP} is measured by fitting for signal yields and (aside from acceptance effects) does not require measuring decay times. For neutral D decays, A_{CP} receives contributions from both direct (in the decay amplitudes) and indirect (due to mixing) processes: $A_{CP}(D^0 \to f) = A^f_{CP} + A^{\rm indirect}_{CP}$. The latter indirect contribution depends on the mixing parameters x and y:

$$A^{\rm indirect}_{CP} \;=\; \frac{1}{2}\left(\left|\frac{q}{p}\right| + \left|\frac{p}{q}\right|\right) x\sin\phi - \frac{1}{2}\left(\left|\frac{q}{p}\right| - \left|\frac{p}{q}\right|\right) y\cos\phi = \; -A_\Gamma\,. \tag{70.43}$$

Numerous measurements of A_{CP} for decays to CP eigenstates are listed in this *Review* [74]. Table 70.6 summarizes the current status of measurements of the *difference* in A_{CP} for $D^0 \to K^+K^-$

and $D^0 \to \pi^+\pi^-$ decays: $\Delta A_{CP} \equiv A_{CP}(K^+K^-) - A_{CP}(\pi^+\pi^-)$. Within the Standard Model, $A_{CP}^{KK} \approx -A_{CP}^{\pi\pi}$ [75], and ΔA_{CP} essentially doubles any direct CP violation present. The difference is also advantageous experimentally, as several systematic uncertainties cancel. As A_{CP}^{indirect} is independent of final state, it subtracts out of ΔA_{CP}. However, at hadron experiments such as LHCb, there is a difference in efficiencies between K^+K^- and $\pi^+\pi^-$ such that $\langle t\rangle_{KK} \neq \langle t\rangle_{\pi\pi}$, i.e., the mean decay times slightly differ. This difference leads to a small contribution to ΔA_{CP} from A_{CP}^{indirect} [72]. The most recent ΔA_{CP} result from LHCb [76], based on 8.9 fb^{-1} of data, differs from zero with a statistical significance of 5.3σ. Thus, this measurement constitutes the first observation of CP violation in charm decays. These CP asymmetries are included in HFLAV's global fit for charm mixing parameters discussed below.

Table 70.6: Results for the difference in time-integrated CP asymmetries ΔA_{CP} between $D^0 \to K^+K^-$ and $D^0 \to \pi^+\pi^-$ decays. When a single uncertainty is listed, that corresponds to statistical and systematic uncertainties combined. The measurements with an asterisk (*) have been either superseded or combined with subsequent results and thus are not included in the HFLAV global fit.

Year	Experiment	ΔA_{CP} ($\times 10^{-3}$)
2019	LHCb (8.9 fb^{-1} B, D^* tags) [76]	-1.54 ± 0.29
2013	CDF (9.7 fb^{-1} D^* tag) [77]	$-6.2 \pm 2.1 \pm 1.0$
2008	BABAR (386 fb^{-1}) [78]	$2.4 \pm 6.2 \pm 2.6$
2008	Belle (540 fb^{-1}) [79]	$-8.6 \pm 6.0 \pm 0.7$
2016*	LHCb (3.0 fb^{-1} D^* tag) [80]	$-1.0 \pm 0.8 \pm 0.3$
2014*	LHCb (3.0 fb^{-1} B tag) [81]	$1.4 \pm 1.6 \pm 0.8$
2013*	LHCb (1.0 fb^{-1} B tag) [82]	$4.9 \pm 3.0 \pm 1.4$
2012*	LHCb (0.62 fb^{-1} D^* tag) [83]	$-8.2 \pm 2.1 \pm 1.1$
2012‡	Belle (976 fb^{-1}) [84]	$-8.7 \pm 4.1 \pm 0.6$

‡This preliminary result was not published and thus is not included in the HFLAV global fit.

70.5 Quantum-correlated $D^0\overline{D}^0$ Analyses

Measurements of R_D, $\cos\delta_{K\pi}$, $\sin\delta_{K\pi}$, x, and y can be obtained from a combined fit to time-integrated yields of single-tagged (ST) and double-tagged (DT) $D^0\overline{D}^0$ events produced at the $\psi(3770)$ resonance. Single-tagged events are those in which either the D^0 or $\overline{D}^0$ decay is reconstructed (identified), and the other neutral D decays generically. Double-tagged events are those in which both the D^0 and $\overline{D}^0$ decays are identified. Due to quantum correlations, the decay of a D^0, $\overline{D}^0$, D_+, or D_- projects the other neutral D into a state $\overline{D}^0$, D^0, D_-, or D_+, respectively. The CP-specific D_- and D_+ decays (or, neglecting CP violation, D_1 and D_2 decays) include interference between D^0 and $\overline{D}^0$ amplitudes, and this provides sensitivity to R_D and $\cos\delta_{K\pi}$. The flavor-specific D^0 and $\overline{D}^0$ decays include interference between D_1 and D_2 amplitudes, and this provides sensitivity to x and y. For details of this method, see Refs. [1–5].

BESIII has reported results using 2.9 fb^{-1} of $e^+e^- \to \psi(3770)$ data, where the quantum-correlated $D^0\overline{D}^0$ pairs are produced in a $C=-1$ state. They measure $y_{CP} = (-2.0 \pm 1.3 \pm 0.7)\%$ [56] from DT yields using a CP-eigenstate tag for one D and a flavor-specific semileptonic tag for the other; and they measure $A_{K\pi}^{CP} = (13.2 \pm 1.1 \pm 0.7)\%$ [85] from DT yields using a CP tag for one D and a $K^\pm\pi^\mp$ tag for the other. For y_{CP}, the CP eigenstates used are K^-K^+ (f_+), $\pi^+\pi^-$ (f_+), $K_S^0\pi^0\pi^0$ (f_+), $K_S^0\pi^0$ (f_-), $K_S^0\eta$ (f_-), and $K_S^0\omega$ (f_-). For $A_{K\pi}^{CP}$, seven additional CP eigenstates are included: $\pi^0\pi^0$ (f_+), $K^0_S\,\eta'$ (f_-), $K^0_S\,\phi$ (f_-), $K^0_L\,\pi^0$ (f_+), $K^0_L\,\omega$ (f_+), $K^0_L\,\pi^0\pi^0$ (f_-), and $\pi^+\pi^-\pi^0$ (mixed CP). Using Eq. (70.29) and external inputs for the CP-even fraction of $D^0 \to \pi^+\pi^-\pi^0$ (from Ref. [86]) and values of R_D and y (from HFLAV [87]), BESIII obtains $\delta_{K\pi} = (7.6\,^{+10.4}_{-11.6})^\circ$ [85].

CLEO-c has reported results using 0.82 fb^{-1} of $e^+e^- \to \psi(3770)$ data [88–90]. The values for y, R_M, $\cos\delta_{K\pi}$, and $\sin\delta_{K\pi}$ are obtained from a combined fit to the ST (hadronic only) and DT yields. The DT yields include events in which one D is reconstructed in a hadronic mode and the other D is partially reconstructed in flavor-specific $D \to K^\mp e^\pm \nu$ and $D \to K^\mp \mu^\pm \nu$ modes. The CLEO-c analysis obtains $\cos\delta_{K\pi} = 0.81\,^{+0.22}_{-0.18}\,^{+0.07}_{-0.05}$ and $\sin\delta_{K\pi} = -0.01 \pm 0.41 \pm 0.04$. These fits allow $\cos\delta_{K\pi}$ and $\sin\delta_{K\pi}$ (and also x^2) to be unphysical. Constraining $\cos\delta_{K\pi}$ and $\sin\delta_{K\pi}$ to the physical range $[-1, +1]$ (i.e., interpreting $\delta_{K\pi}$ as an angle) and also using external inputs for x, y, and y_{CP} from HFLAV 2012 [91], CLEO-c obtains $\delta_{K\pi} = (18\,^{+11}_{-17})^\circ$ [90].

70.6 Summary of Experimental Results

The first evidence for D^0-$\overline{D}^0$ mixing was obtained in 2007 by Belle [69] and BABAR [20]. These results were confirmed by CDF [92] and, much later, by LHCb [22]. There are now numerous measurements of D^0-$\overline{D}^0$ mixing with various levels of sensitivity. For $D^0 \to K^+\pi^-$ decays, LHCb [21,22], CDF [19], and Belle [18] each exclude the no-mixing hypothesis by more than five standard deviations. LHCb [44] reported the observation of charm mixing in $D^0 \to K^+\pi^-\pi^+\pi^-$ decays with 8.2σ significance. However, the strong phase difference for this decay is not known, and thus the mixing parameters x and y cannot be extracted. The most precise measurements of x and y are obtained from a time-dependent Dalitz plot analysis of $D^0 \to K^0_S\,\pi^+\pi^-$ decays. This method was developed at CLEO [93] and subsequently used at Belle [39,41] and BABAR [40] with much higher statistics. BABAR has applied this method also to $D^0 \to K^0_S\,K^+K^-$ decays [40]. It has recently been used by LHCb with very high statistics [34,35] to obtain the most precise values of x and y to date. This measurement resulted in the first observation ($> 5\sigma$ significance) of dispersive mixing ($x \neq 0$).

The experimental measurements establish that D^0 and $\overline{D}^0$ mesons mix. This mixing is presumably dominated by long-distance amplitudes, which are difficult to calculate. Under the assumption that the observed mixing is due entirely to non-Standard Model processes, significant constraints on new physics models can be obtained [94]. A significant limitation to interpreting charm mixing in terms of new physics is the theoretical uncertainty on Standard Model predictions [95, 96]. We note that the HFLAV global fit results for x and y (see below) indicate that charm mixing is at the upper end of the range of these predictions. The current situation would benefit from knowledge of the strong phase difference $\delta_{K\pi\pi}$ between $\overline{D}^0 \to K^+\pi^-\pi^0$ and $D^0 \to K^+\pi^-\pi^0$ decays, and similarly the strong phase difference $\delta_{K\pi\pi\pi}$ between $\overline{D}^0 \to K^+\pi^-\pi^+\pi^-$ and $D^0 \to K^+\pi^-\pi^+\pi^-$ decays. Such knowledge would allow one to extract x and y from measurements of (x''^2, y'') and $(x''^2_{K3\pi}, y''_{K3\pi})$ for these three- and four-body decays.

With regard to CP violation, by combining four separate measurements from two data sets totalling 8.9 fb^{-1} of data, LHCb observed CP violation in D decays for the first time [76]. The observable measured is the difference $\Delta A_{CP} = A_{CP}(K^+K^-) - A_{CP}(\pi^+\pi^-)$, which is dominated by *direct* CP violation, i.e., the potential contributions from indirect CP violation mostly cancel. The amount of direct CP violation observed is small: $\Delta A_{CP} = (-0.154 \pm 0.029)\%$. A theory calculation indicates this value is consistent with Standard Model expectations [97]; however, new physics contributions cannot be excluded. A subsequent LHCb measurement of $A_{CP}(K^+K^-) = (0.068 \pm 0.056)\%$ differs from zero by only 1.2σ [98]; thus, the ΔA_{CP} result is interpreted as indicating direct CP violation in $D^0 \to \pi^+\pi^-$ decays.

70.7 HFLAV Global Fit for Charm Mixing Parameters

The Heavy Flavor Averaging Group (HFLAV) performs global fits to all relevant mixing measurements to obtain world average values for the following parameters: mixing parameters x and y; strong phase differences $\delta_{K\pi}$ and $\delta_{K\pi\pi^0}$; the ratio R_D of $D^0 \to K^+\pi^-$ and $\overline{D}^0 \to K^+\pi^-$ partial widths; direct CP-violating parameters $A_D(K^+\pi^-)$, $A_{CP}^{KK} \equiv A_K$, and $A_{CP}^{\pi\pi} \equiv A_\pi$; and indirect CP-violating parameters $|q/p|$, $\mathrm{Arg}(q/p) \equiv \phi$, ϕ_{12}, ϕ_2^M, and ϕ_2^Γ. Four separate fits are performed: *(a)* assuming no CP violation; *(b)* assuming no subleading amplitudes for indirect CP violation; *(c)* assuming no subleading amplitudes in Cabibbo-favored and doubly Cabibbo-suppressed decays; and *(d)* allowing for all CP violation. Fits *(b)* and *(c)* correspond to theory expectations [73, 99, 100], with the latter being less restrictive. For fit *(b)*, four fitted parameters are reduced to three using the relationship $\tan\phi = (x/y)\cdot(1-|q/p|^2)/(1+|q/p|^2)$ [99–101]; alternatively, one can fit for the three parameters $x_{12} \equiv 2|M_{12}|/\Gamma$, $y_{12} \equiv |\Gamma_{12}|/\Gamma$, and $\phi_{12} \equiv \mathrm{Arg}(M_{12}/\Gamma_{12})$, from which x, y, $|q/p|$, and ϕ can be derived. Details of these fits are given in Ref. [87].

Table 70.7: HFLAV global fit results (see text) [15].

Parameter	No CP violation Fit *(a)*	No subleading amplitudes for indirect CPV Fit *(b)*	No subleading amplitudes in CF+DCS decays Fit *(c)*	All CP violation allowed Fit *(d)*	95% C.L. Interval (CPV allowed)
x (%)	$0.434^{+0.126}_{-0.139}$	0.407 ± 0.044	–	0.407 ± 0.044	[0.320, 0.493]
y (%)	0.646 ± 0.024	$0.643^{+0.024}_{-0.023}$	–	$0.645^{+0.024}_{-0.023}$	[0.600, 0.692]
$\delta_{K\pi}$ (°)	$11.5^{+3.6}_{-3.7}$	$11.3^{+3.6}_{-3.8}$	$10.9^{+3.6}_{-3.8}$	$11.4^{+3.5}_{-3.8}$	[3.7, 18.2]
R_D (%)	0.344 ± 0.002	0.344 ± 0.002	0.344 ± 0.002	0.344 ± 0.002	[0.340, 0.347]
A_D (%)	–	–	–	-0.77 ± 0.35	[−1.46, −0.08]
$\|q/p\|$	–	1.005 ± 0.007	–	$0.994^{+0.016}_{-0.015}$	[0.96, 1.02]
ϕ (°)	–	-0.19 ± 0.26	–	$-2.6^{+1.1}_{-1.2}$	[−4.88, −0.37]
$\delta_{K\pi\pi}$ (°)	$23.1^{+22.8}_{-23.2}$	$24.5^{+21.4}_{-22.5}$	$24.4^{+21.5}_{-22.5}$	$24.6^{+21.4}_{-22.5}$	[−20.1, 65.7]
A_π(%)	–	0.202 ± 0.059	0.200 ± 0.059	0.218 ± 0.060	[0.10, 0.34]
A_K(%)	–	0.045 ± 0.053	0.043 ± 0.053	0.062 ± 0.054	[−0.04, 0.17]
x_{12} (%)	–	0.407 ± 0.044	0.407 ± 0.044	–	[0.321, 0.494]
y_{12} (%)	–	$0.643^{+0.024}_{-0.023}$	$0.641^{+0.024}_{-0.023}$	–	[0.595, 0.687]
ϕ_{12}(°)	–	$0.65^{+0.92}_{-0.90}$	–	–	[−1.13, 2.49]
ϕ_2^M(°)	–	–	0.48 ± 0.92	–	[−1.35, 2.32]
ϕ_2^Γ(°)	–	–	$2.40^{+1.55}_{-1.54}$	–	[−0.61, 5.45]
χ^2/d.o.f.	100.6/(63−5) = 1.74	68.9/(63−8) = 1.25	66.5/(63−9) = 1.23	65.4/(63−10) = 1.23	

The fits use Belle, BABAR, CDF, and LHCb measurements of $D^0 \to K^{(*)+}\ell^-\overline{\nu}$, K^+K^-, $\pi^+\pi^-$, $K^+\pi^-$, $K^+\pi^-\pi^0$, $K^+\pi^-\pi^+\pi^-$, $K_S^0\pi^+\pi^-$, $K_S^0K^+K^-$, and $\pi^+\pi^-\pi^0$ decays, as well as CLEO-c and BESIII measurements of $\cos\delta$, $\sin\delta$, and $A_{CP}(K^+\pi-)$ obtained from quantum-correlated branching fractions measured in $e^+e^- \to \psi(3770) \to D^0\overline{D}^0$ reactions. Correlations among observables are taken into account by using the error matrices provided by the experiments. Three observables input to the fit are themselves world average values calculated by HFLAV: $R_M = (x^2+y^2)/2$ from $D^0 \to K^{(*)+}\ell^-\overline{\nu}$ decays (Table 70.1), and y_{CP} and A_Γ from $D^0 \to f_{CP}$ decays (Table 70.5). A measurement by LHCb of R_M using $D^0 \to K^+\pi^-\pi^+\pi^-$ decays is input separately.

The results of the fit as of September, 2023 are listed in Table 70.7. Confidence contours in the two dimensions (x, y) and $(|q/p|, \phi)$ resulting from the fit are plotted in Fig. 70.1. These contours are obtained by allowing, for any point in the two-dimensional plane, all other fitted parameters to take their preferred values. The 1σ–5σ boundaries drawn are the loci of points in which the χ^2 has risen above the minimum by 2.30, 6.18, 11.83, 19.33, and 28.67 units. The fit excludes the no-mixing point $x = y = 0$ at more than 11.5σ. The fit is consistent with CP conservation ($|q/p| = 1$, $\phi = 0$) at the 2σ level. The χ^2 of the all-CP-violation-allowed fit is 65.4 for $63-10 = 53$ degrees of freedom, which is satisfactory. One-dimensional likelihood functions for parameters are obtained by allowing, for any value of the parameter, all other fitted parameters to take their preferred values. The resulting likelihood functions give central values, 68.3% C.L. intervals, and 95% C.L. intervals as listed in Table 70.7.

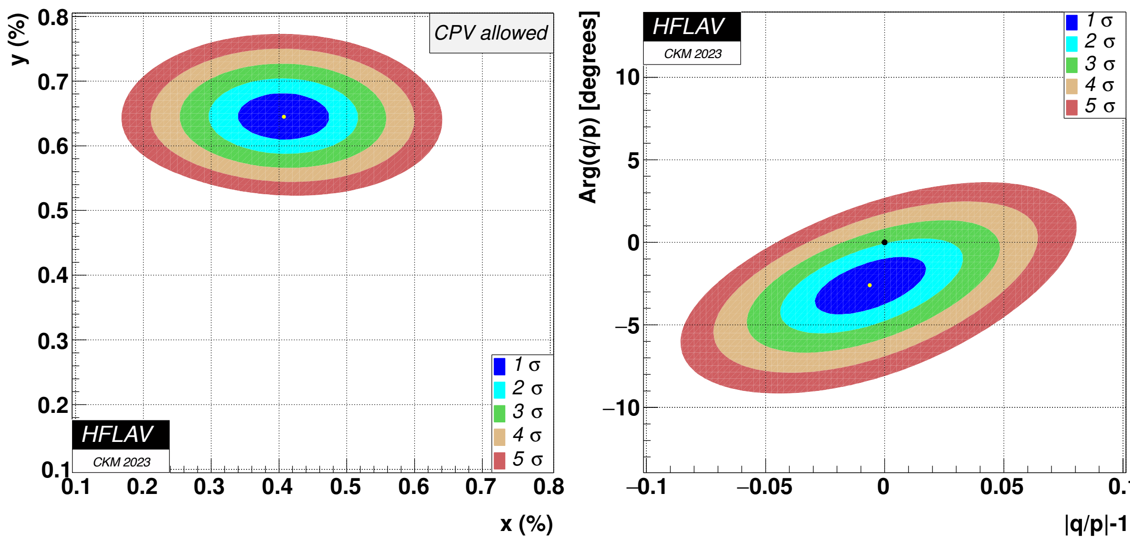

Figure 70.1: Two-dimensional 1σ-5σ contours for (x, y) (left) and for $(|q/p|, \text{Arg}(q/p))$ (right) as obtained by HFLAV [15]. In the right plot, the black dot denotes the no-CP-violation point $(0, 0)$.

From the results of the HFLAV global fit, we conclude the following: (1) Since CP violation is small and y_{CP} is positive, the CP-even state is shorter-lived, as in the $K^0\overline{K}^0$ system. (2) Since x is positive, the CP-even state is heavier, unlike in the $K^0\overline{K}^0$ system. (3) The strong phase difference $\delta_{K\pi}$ is small but probably nonzero: the 95% C.L. interval is $3.7^\circ < \delta_{K\pi} < 18.2^\circ$. (4) While direct CP violation has been observed in D decays, there is still no evidence for indirect CP violation, i.e., $|q/p| \neq 1$ or $\phi \neq 0$. Observing such CP violation at the current level of sensitivity would indicate new physics.

70.8 Future Data

Current results are based primarily upon CLEO-c (0.82 fb^{-1} of $e^+e^- \to \psi(3770)$ data), Belle and BABAR ($\sim$1.4 ab^{-1} of $e^+e^- \to \Upsilon(4S)$ data), CDF (9.6 fb^{-1} of $p\bar{p}$ collision data at $\sqrt{s} = 1.96$ TeV), and LHCb Runs 1 and 2 (3.0 fb^{-1}+ 5.9 fb^{-1} of pp collision data at $\sqrt{s} = 7$, 8, 13 TeV).

BESIII has accumulated 8 fb^{-1} of $e^+e^- \to \psi(3770)$ data and plans to collect a total of 20 fb^{-1} by 2025. These data should provide strong phase measurements that would enable improved model-independent determinations of mixing parameters from Belle II and LHCb. In 2019, Belle II began accumulating 50 ab^{-1} of $e^+e^- \to \Upsilon(4S)$ data [102], which is expected to take approximately ten years to collect. At LHCb, Run 2 was completed in 2018, Run 3 is now in progress, and Run 4 is planned for 2027-30 [103]. The goal for Runs $3+4$ is to accumulate an additional 50 fb^{-1} of pp data at $\sqrt{s} \approx 14$ TeV [104]. These data, along with the large e^+e^- dataset from Belle II, should provide more precise measurements of D^0-$\overline{D}^0$ mixing and direct CP violation, and might possibly uncover indirect CP violation in the neutral D system.

References

[1] D. M. Asner and W. M. Sun, Phys. Rev. **D73**, 034024 (2006), [Erratum: Phys. Rev. **D77**, 019901 (2008)], [hep-ph/0507238].

[2] D. Atwood and A. A. Petrov, Phys. Rev. **D71**, 054032 (2005), [hep-ph/0207165].

[3] M. Gronau, Y. Grossman and J. L. Rosner, Phys. Lett. **B508**, 37 (2001), [hep-ph/0103110].

[4] Z.-z. Xing, Phys. Rev. **D55**, 196 (1997), [hep-ph/9606422].

[5] M. Goldhaber and J. L. Rosner, Phys. Rev. **D15**, 1254 (1977).

[6] Y. S. Amhis *et al.* (HFLAV), Eur. Phys. J. C **81**, 3, 226 (2021), [arXiv:1909.12524].

[7] U. Bitenc *et al.* (Belle), Phys. Rev. **D77**, 112003 (2008), [arXiv:0802.2952].

[8] B. Aubert *et al.* (BaBar), Phys. Rev. **D76**, 014018 (2007), [arXiv:0705.0704].

[9] C. Cawlfield *et al.* (CLEO), Phys. Rev. **D71**, 077101 (2005), [hep-ex/0502012].

[10] E. M. Aitala *et al.* (E791), Phys. Rev. Lett. **77**, 2384 (1996), [hep-ex/9606016].

[11] U. Bitenc *et al.* (Belle), Phys. Rev. **D72**, 071101 (2005), [hep-ex/0507020].

[12] B. Aubert *et al.* (BaBar), Phys. Rev. **D70**, 091102 (2004), [hep-ex/0408066].

[13] Y. Nir, Lectures given at 27th SLAC Summer Institute on Particle Physics: "CP Violation in and Beyond the Standard Model (SSI 99)," Stanford, California, 7-16 July 1999. Published in Trieste 1999, *Particle Physics*, pp. 165-243.

[14] S. Bergmann *et al.*, Phys. Lett. **B486**, 418 (2000), [hep-ph/0005181].

[15] Heavy Flavor Averaging Group, `https://hflav-eos.web.cern.ch/hflav-eos/charm/CKM23/results_mix_cpv.html`.

[16] R. Aaij *et al.* (LHCb), Phys. Rev. **D97**, 3, 031101 (2018), [arXiv:1712.03220].

[17] R. Aaij *et al.* (LHCb), Phys. Rev. **D95**, 5, 052004 (2017), [Erratum: Phys. Rev. **D96**, 099907 (2017)], [arXiv:1611.06143].

[18] B. R. Ko *et al.* (Belle), Phys. Rev. Lett. **112**, 11, 111801 (2014), [Addendum: Phys. Rev. Lett. **112**, 139903 (2014)], [arXiv:1401.3402].

[19] T. A. Aaltonen *et al.* (CDF), Phys. Rev. Lett. **111**, 23, 231802 (2013), [arXiv:1309.4078].

[20] B. Aubert *et al.* (BaBar), Phys. Rev. Lett. **98**, 211802 (2007), [hep-ex/0703020].

[21] R. Aaij *et al.* (LHCb), Phys. Rev. Lett. **111**, 25, 251801 (2013), [arXiv:1309.6534].

[22] R. Aaij *et al.* (LHCb), Phys. Rev. Lett. **110**, 10, 101802 (2013), [arXiv:1211.1230].

[23] T. Aaltonen *et al.* (CDF), Phys. Rev. Lett. **100**, 121802 (2008), [arXiv:0712.1567].

[24] L. M. Zhang *et al.* (Belle), Phys. Rev. Lett. **96**, 151801 (2006), [hep-ex/0601029].

[25] J. M. Link *et al.* (FOCUS), Phys. Lett. **B618**, 23 (2005), [hep-ex/0412034].

[26] R. Godang *et al.* (CLEO), Phys. Rev. Lett. **84**, 5038 (2000), [hep-ex/0001060].

[27] E. M. Aitala *et al.* (E791), Phys. Rev. **D57**, 13 (1998), [hep-ex/9608018].

[28] M. Ablikim *et al.* (BESIII), Phys. Lett. **B734**, 227 (2014), [arXiv:1404.4691].

[29] See "Review of Multibody Charm Analyses" in this *Review*.

[30] B. Aubert *et al.* (BaBar), Phys. Rev. Lett. **97**, 221803 (2006), [hep-ex/0608006].

[31] B. Aubert *et al.* (BaBar), Phys. Rev. Lett. **103**, 211801 (2009), [arXiv:0807.4544].

[32] J. Libby *et al.* (CLEO), Phys. Rev. **D82**, 112006 (2010), [arXiv:1010.2817].

[33] A. Di Canto *et al.*, Phys. Rev. **D99**, 1, 012007 (2019), [arXiv:1811.01032].
[34] R. Aaij *et al.* (LHCb), Phys. Rev. D **108**, 052005 (2023), [arXiv:2208.06512].
[35] R. Aaij *et al.* (LHCb), Phys. Rev. Lett. **127**, 11, 111801 (2021), [arXiv:2106.03744].
[36] R. Aaij *et al.* (LHCb), Phys. Rev. Lett. **122**, 23, 231802 (2019), [arXiv:1903.03074].
[37] R. Aaij *et al.* (LHCb), JHEP **04**, 033 (2016), [arXiv:1510.01664].
[38] J. P. Lees *et al.* (BaBar), Phys. Rev. **D93**, 11, 112014 (2016), [arXiv:1604.00857].
[39] T. Peng *et al.* (Belle), Phys. Rev. **D89**, 9, 091103 (2014), [arXiv:1404.2412].
[40] P. del Amo Sanchez *et al.* (BaBar), Phys. Rev. Lett. **105**, 081803 (2010), [arXiv:1004.5053].
[41] K. Abe *et al.* (Belle), Phys. Rev. Lett. **99**, 131803 (2007), [arXiv:0704.1000].
[42] D. M. Asner *et al.* (CLEO), Phys. Rev. **D72**, 012001 (2005), [hep-ex/0503045].
[43] E. White *et al.* (Belle), Phys. Rev. **D88**, 5, 051101 (2013), [arXiv:1307.5935].
[44] R. Aaij *et al.* (LHCb), Phys. Rev. Lett. **116**, 24, 241801 (2016), [arXiv:1602.07224].
[45] H. Muramatsu *et al.* (CLEO), Phys. Rev. Lett. **89**, 251802 (2002), [Erratum: Phys. Rev. Lett. **90**, 059901 (2003)], [hep-ex/0207067].
[46] M. Ablikim *et al.* (BESIII), Phys. Rev. D **101**, 11, 112002 (2020), [arXiv:2003.00091].
[47] B. Aubert *et al.* (BaBar), Phys. Rev. Lett. **95**, 121802 (2005), [hep-ex/0504039].
[48] B. Aubert *et al.* (BaBar), Phys. Rev. **D78**, 034023 (2008), [arXiv:0804.2089].
[49] R. Aaij *et al.* (LHCb), Phys. Rev. D **105**, 9, 092013 (2022), [arXiv:2202.09106].
[50] R. Aaij *et al.* (LHCb), Phys. Rev. D **104**, 7, 072010 (2021), [arXiv:2105.09889].
[51] M. Nayak *et al.* (Belle), Phys. Rev. D **102**, 7, 071102 (2020), [arXiv:1912.10912].
[52] R. Aaij *et al.* (LHCb), Phys. Rev. Lett. **122**, 1, 011802 (2019), [arXiv:1810.06874].
[53] R. Aaij *et al.* (LHCb), Phys. Rev. Lett. **118**, 26, 261803 (2017), [arXiv:1702.06490].
[54] M. Starič *et al.* (Belle), Phys. Lett. **B753**, 412 (2016), [arXiv:1509.08266].
[55] R. Aaij *et al.* (LHCb), JHEP **04**, 043 (2015), [arXiv:1501.06777].
[56] M. Ablikim *et al.* (BESIII), Phys. Lett. **B744**, 339 (2015), [arXiv:1501.01378].
[57] T. A. Aaltonen *et al.* (CDF), Phys. Rev. **D90**, 11, 111103 (2014), [arXiv:1410.5435].
[58] J. P. Lees *et al.* (BaBar), Phys. Rev. **D87**, 1, 012004 (2013), [arXiv:1209.3896].
[59] A. Zupanc *et al.* (Belle), Phys. Rev. **D80**, 052006 (2009), [arXiv:0905.4185].
[60] S. E. Csorna *et al.* (CLEO), Phys. Rev. **D65**, 092001 (2002), [hep-ex/0111024].
[61] J. M. Link *et al.* (FOCUS), Phys. Lett. **B485**, 62 (2000), [hep-ex/0004034].
[62] E. M. Aitala *et al.* (E791), Phys. Rev. Lett. **83**, 32 (1999), [hep-ex/9903012].
[63] Heavy Flavor Averaging Group, `https://hflav-eos.web.cern.ch/hflav-eos/charm/CKM23/results_mixing.html`.
[64] R. Aaij *et al.* (LHCb), Phys. Rev. **D101**, 1, 012005 (2020), [arXiv:1911.01114].
[65] R. Aaij *et al.* (LHCb), Phys. Rev. Lett. **112**, 4, 041801 (2014), [arXiv:1310.7201].
[66] R. Aaij *et al.* (LHCb), JHEP **04**, 129 (2012), [arXiv:1112.4698].
[67] B. Aubert *et al.* (BaBar), Phys. Rev. **D80**, 071103 (2009), [arXiv:0908.0761].
[68] B. Aubert *et al.* (BaBar), Phys. Rev. **D78**, 011105 (2008), [arXiv:0712.2249].
[69] M. Staric *et al.* (BELLE), Phys. Rev. Lett. **98**, 211803 (2007), [,65(2007)], [hep-ex/0703036].
[70] B. Aubert *et al.* (BaBar), Phys. Rev. Lett. **91**, 121801 (2003), [hep-ex/0306003].

[71] K. Abe *et al.* (Belle), Phys. Rev. Lett. **88**, 162001 (2002), [hep-ex/0111026].
[72] M. Gersabeck *et al.*, J. Phys. G **39**, 045005 (2012), [arXiv:1111.6515].
[73] A. L. Kagan and L. Silvestrini, Phys. Rev. D **103**, 5, 053008 (2021), [arXiv:2001.07207].
[74] See the tabulation of A_{CP} results in the D^0 and D^+ Listings in this *Review*.
[75] Y. Grossman, A. L. Kagan and Y. Nir, Phys. Rev. D **75**, 036008 (2007), [hep-ph/0609178].
[76] R. Aaij *et al.* (LHCb), Phys. Rev. Lett. **122**, 21, 211803 (2019), [arXiv:1903.08726].
[77] T. Aaltonen *et al.* (CDF), Phys. Rev. Lett. **109**, 111801 (2012), [arXiv:1207.2158].
[78] B. Aubert *et al.* (BaBar), Phys. Rev. Lett. **100**, 061803 (2008), [arXiv:0709.2715].
[79] M. Staric *et al.* (Belle), Phys. Lett. **B670**, 190 (2008), [arXiv:0807.0148].
[80] R. Aaij *et al.* (LHCb), Phys. Rev. Lett. **116**, 19, 191601 (2016), [arXiv:1602.03160].
[81] R. Aaij *et al.* (LHCb), JHEP **07**, 041 (2014), [arXiv:1405.2797].
[82] R. Aaij *et al.* (LHCb), Phys. Lett. **B723**, 33 (2013), [arXiv:1303.2614].
[83] R. Aaij *et al.* (LHCb), Phys. Rev. Lett. **108**, 111602 (2012), [arXiv:1112.0938].
[84] B. R. Ko (Belle), in "7th International Workshop on the CKM Unitarity Triangle (CKM 2012) Cincinnati, Ohio, USA, September 28-October 2, 2012," (2012), [arXiv:1212.5320].
[85] M. Ablikim *et al.* (BESIII), Eur. Phys. J. C **82**, 11, 1009 (2022), [arXiv:2208.09402].
[86] S. Malde *et al.*, Phys. Lett. B **747**, 9 (2015), [arXiv:1504.05878].
[87] Y. S. Amhis *et al.* (Heavy Flavor Averaging Group, HFLAV), Phys. Rev. D **107**, 5, 052008 (2023), [arXiv:2206.07501].
[88] J. L. Rosner *et al.* (CLEO), Phys. Rev. Lett. **100**, 221801 (2008), [arXiv:0802.2264].
[89] D. M. Asner *et al.* (CLEO), Phys. Rev. **D78**, 012001 (2008), [arXiv:0802.2268].
[90] D. M. Asner *et al.* (CLEO), Phys. Rev. **D86**, 112001 (2012), [arXiv:1210.0939].
[91] Heavy Flavor Averaging Group, `https://hflav-eos.web.cern.ch/hflav-eos/charm/March12/results_mix_cpv.html`.
[92] T. Aaltonen *et al.* (CDF), Phys. Rev. Lett. **100**, 121802 (2008), [arXiv:0712.1567].
[93] D. M. Asner *et al.* (CLEO), Phys. Rev. D **72**, 012001 (2005), [hep-ex/0503045].
[94] E. Golowich *et al.*, Phys. Rev. **D76**, 095009 (2007), [arXiv:0705.3650].
[95] G. Isidori *et al.*, Phys. Lett. **B711**, 46 (2012), [arXiv:1111.4987].
[96] E. Franco, S. Mishima and L. Silvestrini, JHEP **05**, 140 (2012), [arXiv:1203.3131].
[97] J. Brod, A. L. Kagan and J. Zupan, Phys. Rev. D **86**, 014023 (2012), [arXiv:1111.5000].
[98] R. Aaij *et al.* (LHCb), Phys. Rev. Lett. **131**, 9, 091802 (2023), [arXiv:2209.03179].
[99] Y. Grossman, Y. Nir and G. Perez, Phys. Rev. Lett. **103**, 071602 (2009), [arXiv:0904.0305].
[100] A. L. Kagan and M. D. Sokoloff, Phys. Rev. **D80**, 076008 (2009), [arXiv:0907.3917].
[101] M. Ciuchini *et al.*, Phys. Lett. **B655**, 162 (2007), [hep-ph/0703204].
[102] W. Altmannshofer *et al.* (Belle-II), PTEP **2019**, 12, 123C01 (2019), [Erratum: PTEP 2020, 029201 (2020)], [arXiv:1808.10567].
[103] CERN LHC Schedule, `https://lhc-commissioning.web.cern.ch/schedule/LHC-long-term.htm`.
[104] R. Aaij *et al.* (LHCb) (2018), [arXiv:1808.08865].